Heritage Science

RESEARCH

Open Access

Key characterization efforts to support the graffiti ink removal and care of Mark Rothko's painting 'Black on Maroon' 1958

Scott T. Wills[1], Bronwyn A. Ormsby[2*], Melinda H. Keefe[3] and Robert L. Sammler[4]

Abstract

Analytical characterization efforts carried out in support of the conservation treatment of Mark Rothko's painting 'Black on Maroon' 1958 (Tate T01170), involving the removal of graffiti (tag) ink, are summarized. The proprietary ink product, of unfamiliar and unknown composition, was investigated using a suite of analytical techniques (IR spectroscopy, GC–MS, ICP-MS, pyrolysis GC–MS, thin layer chromatography, SEC, MALDI-TOF–MS, and UHPLC-MS) to identify key colorants and other components. The ink solubility properties proved vital to informing the solvent selection process for the ink removal procedure, which helped enable the re-display of the painting at Tate Modern in 2014. The possible impact of ink residues remaining within the cotton duck canvas support of the conserved painting was also explored using mockup canvas mechanical strength data, measured before and after 'soiling' at two ink levels to assess whether the ink residues had any immediate and possible longer-term effects on canvas properties. These findings, elucidated using a range of complementary analytical techniques, provide information on this hitherto-unknown graffiti product, contribute to a growing body of knowledge in this area, and offer analytical approaches which may be useful for the characterization of similar unknown materials, whether used to damage, augment, or create works of art.

Keywords: Graffiti, Ink, Analysis, Removal, Solubility, Rothko, Tensile strength

Introduction

One of the series of nine Seagram Mural paintings, created and later donated to Tate by Mark Rothko (1903–1970), 'Black on Maroon', 1958 (T01170) (Fig. 1), was damaged with an ink-based graffiti product during an incident at Tate Modern in 2012. The damage naturally posed a significant conservation challenge as the underlying paint layers are delicate, made from a complex range of organic and inorganic paint and coating materials, and are intentionally unprotected by an overall varnish layer. In addition, the ink itself was—at the time of the incident—an unknown quantity. Remediation therefore required sophisticated collaborative conservation, analytical, material and heritage science expertise.

The eighteen-month conservation project that followed consisted of three key stages. Firstly, the research phase which involved (a) a thorough technical examination of the painting and a review of previous analytical campaigns, as well as initial analytical characterization of the ink product used, (b) the creation of relevant treatment test (representative) samples based on the known painting layer structure and materials, and (c) the development and refinement of an ink removal process which was evaluated and finely tuned prior to carrying out the first discrete tests on the painting [1, 2]. This was followed by two stages of active conservation treatment: the ink removal phase where the bulk of the ink material was removed from the paint layers, followed by a retouching, or surface reintegration, phase. Previous publications

*Correspondence: Bronwyn.Ormsby@tate.org.uk

[2] Conservation Department, Tate Britain, Millbank, Pimlico, London, UK
Full list of author information is available at the end of the article

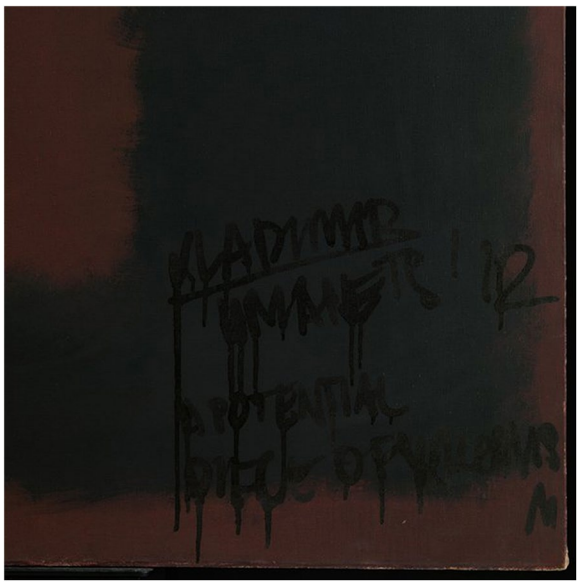

Fig. 1 Image of the lower right corner of the painting 'Black on Maroon' 1958 (Tate T01170) showing the dark, applied tag ink. Image Tate, © Kate Rothko Prizel and Christopher Rothko, 2012

detail the preparation of a testing mock-up/representative sample [2], the initial ink solubility and characterization research [1] and the broad analytical, philosphical and technical approach employed to support this high profile and complex conservation treatment [3]. The current paper presents a detailed account of the extensive scientific characterization of this unknown, proprietary ink material, including ink constituents (dyes and/or pigments, polymers, dispersants, additives, solvents) as well as ink solubility exploration. Finally, as the ink, in some areas, had penetrated through the painting structure—and as removing these residues posed an unacceptable risk to the work of art—an exploration into the possible legacy of leaving ink within the painting and canvas structure was also explored.

Similar to other Rothko works, Black on Maroon is a sophisticated, multi-layered painting on cotton duck canvas containing paints and coatings made from various natural and synthetic resins/polymers including; animal glue, egg, dammar, modified phenol formaldehyde, oil-modified alkyd and other media, all applied in very thin layers with a considerable amount of blending upon subsequent applications [4]. The areas directly affected by the ink material (see Fig. 1) included portions of the mostly uncoated (or unglazed), porous and heavily oxidized maroon paint (containing cadmium red, lithol red [PR49] and ultramarine blue pigment, etc.) as well as the oxidized black 'figure' paint (containing bone and Mars blacks and extenders, etc.), the latter having also been selectively egg and dammar resin-glazed [2, 4].

The ink-based product used during the incident was identified through police reports as Molotow Masterpiece™ Coversall Cocktail ink; described by the manufacturer as alcohol-based, high covering, 100% buff-resistant, ultraviolet light (UV) resistant, quick drying, permanent, and weatherproof [5]. The color is listed as 'signal black', which generally refers to a RAL 9004 industry standard [6]. The general manufacturer descriptions taken from the bottle label include 'synthetic bitumen' and 'viscoplastic coating.' The product was applied via an ink-filled plastic reservoir with a sponge-foam tip in a fluid, dripping state. Bottles of the same product were purchased soon after the incident for testing, which facilitated a prolonged study into this material and its properties. An SDS sheet was provided only after the painting had been re-displayed, which only listed the (by that stage already identified) flammable components of the formulation and a blue solvent dye [1, 2, 7].

Within the first phase of the conservation project, understanding the graffiti ink solubility properties was the highest research priority as this directly informed the development of an ink removal strategy; pragmatically the elucidation of the exact ink constituents could be carried out more fully once the removal process was successfully underway. The ink solubility characterization method utilized commonly applied Hansen's solubility parameters which describes a solute's ability to dissolve in a solvent or solvent blend using four physical properties determined experimentally through regression of solubility data in many known solvents. The four physical properties are dispersion, polar, hydrogen bonding, and radius of interaction. Using these interactions, Relative Cohesive Energy Difference (RED) values were calculated to predict the dried ink's likelihood to dissolve in a broad range of solvents and solvent blends. These predictions supported the design of a tailored solvent blend cleaning system which was evaluated and employed in the conservation treatment. For the post-display phase of the research, the ink material was explored further to determine the constituents more accurately and fully. This involved separation where possible into constituent components and analysis aimed at solvent, colorant, additive and polymeric composition characterization using various forms of spectroscopy, chromatography, and mass spectrometry.

Once the ink had been more fully elucidated, tensile testing was carried out on mockup canvases to determine whether the ink remaining within the painting canvas may have altered the stiffness or brittleness of the fibers or created significant differential tension between the ink-affected and non-affected areas (though no tension-induced distortion has ever been visible around the

affected areas on the painting and canvas). As paintings on canvas supports have inherent vulnerabilities as they age which can largely be attributed to the hydrolysis and oxidation of the cellulose-based fibers, which manifest as loss of molecular weight and increasing acidity with concomitant loss of strength, tension and flexibility [8], it was important to explore whether the affected areas of canvas may have been compromised by the ink beyond the permanent staining effect of the colorants.

This research offers a critical addition to the technical literature in graffiti material characterization and removal which to date has largely focused on spray paints [9, 10]. This will support future technical research and conservation treatment development where this, or similar classes of solvent-based highly staining graffiti ink, have been used on works of art. The results inform the heritage field of the likely composition of similar products and the methodology provides potentially useful analytical approaches for the identification and characterization of similar materials [3].

Experimental

The choice of investigative techniques used was largely informed through the immediacy of established materials identification analytical techniques such as infrared spectroscopy and gas chromatography-mass spectrometry, many of which have been used for spray paint graffiti material characterization [11–14]. However, in this case, as the ink was both novel and relatively abundant, other less commonly employed separation techniques were also used to explore the presence of specific colorants, any polymeric content and the presence of any cross-linked polymeric fraction, in addition to the tensile testing applied to mock-up inked cotton duck canvas samples.

Ink materials

Molotow Masterpiece™ Coversall Cocktail ink was obtained shortly after the incident from the online Molotow site [5]. Dye standards were based on elucidation from earlier studies carried out within the timeframe of the conservation project [1], further analysis within this study and the SDS sheet provided by the manufacturer after the conservation treatment had been completed. The dyes were purchased from Mistral Industrial Chemicals, UK (Solvent Black 5 – Constitution number 50415, Nigrosine spirit soluble, CAS 11099-03-9) [15]; FastColors LLP, UK (Solvent Black 7 – fat soluble nigrosine (phenazine) base, Constitution number 50415:1, CAS 8005–02-5) [16]; and Kremer Pigments, Germany (Solvent Blue 70 – metal complex solvent-soluble phthalocyanine, Constitution number 743530, CAS 12237–24-0) [17]. All solvents used were HPLC grade, purchased from Fisher Scientific, USA.

Infrared spectroscopy

FTIR spectroscopy measurements of the ink were executed to obtain high-level constituent information using a Thermo Nicolet 6700 FTIR equipped with an MCT/B detector and KBr beamsplitter containing a SensIR Technologies DuraSamplIR II ATR accessory (SensIR Technologies). The ink was prepared by drying in a fume hood, then pressing the dried residue onto the ATR crystal; dye powder standards were pressed onto the crystal without additional preparation. All spectra were obtained at ambient temperature over the range 650–4000 cm^{-1}, with a resolution of 4 cm^{-1} and coadding 32 scans.

Pyrolysis gas chromatography-mass spectrometry

Pyrolysis GC–MS of the ink was used to explore the dyes and any polymeric fraction and executed using a Frontier py2020iD pyrolyzer interfaced to a Thermo Trace Ultra GC with DSQII Mass Spectrometer. Pyrolysis was carried out at a furnace temperature of 550 °C. GC conditions: 40:1 split injection, column flow 1.2 mL He/min, 45 °C for 3 min; ramp at 10 °C/min to 120 °C; ramp at 20 °C/min to 320 °C; and hold at 320 °C for 3 min. Column: Restek RTX-5Sil MS (30 m long, 0.25 mm ID, 0.25 µm film thickness). MS conditions: EI mode, scan 25–500 amu every 0.15 s.

Gas chromatography-mass spectrometry

Liquid injection GC–MS was performed on the ink diluted to 1% in acetonitrile to explore the solvent composition, using an Agilent 6890 GC with a quadrupole MS detector. The column used was a Restek RTX-5MS (L = 30 m, ID = 0.32 mm, Df 1 µL). Oven conditions were 50 °C for 5 min then 15 °C/min to 300 °C, with final hold of 5 min. The MS scan range was *m/z* 35–500.

Matrix assisted laser desorption ionization time of flight mass spectrometry

The Bruker Ultraflex MALDI-TOF mass spectrometer was used to compare the ions generated from the ink with those from Solvent Black 7, and to look for ions not otherwise explained by the other techniques. The instrument was configured to operate in reflectron mode and to analyze positively charged ions. The sample was dissolved in THF, mixed 20:1 with a dihydrobenzoic acid matrix and spotted onto a polished steel plate. The sample was ablated with a 337 nm N2 laser operated at a repetition rate of 16.7 Hz. The laser was attenuated to ~ 35% of its maximum power to achieve an optimal balance of ionization efficiency and mass resolution. Each saved mass spectrum was created from an average of 500 laser shots collected from random areas on the sample spot and calibrated using a 2000 Mw poly (methyl methacrylate) standard spotted onto an adjacent cell on the plate. The spectral range was *m/z* 100–5120, with ions below *m*/z

500 suppressed to avoid saturation of the detector from matrix ions.

ICP-MS

The wet ink was analyzed using ICP-MS to determine the metallic constituents of the organometallic dyes present. The sample was prepared in triplicate using approximately 0.1 g in 5 mL 55% nitric acid and digested for one hour in a Milestone Ultrawave microwave digestion system. The samples were then diluted to 15 g in water and analyzed in duplicate on an Agilent 7500 ICP-MS, bracketed with a ladder of matrix-matched standards.

Thin layer chromatography

TLC was carried out to explore the numbers and types of dyes used in the ink, using Whatman LK5F silica gel 150A plates (5 × 20 cm, layer thickness 250 µm) at ambient temperature. Eluents used were as follows: Eluent 1: 90:10 $MeCl_2$: Methanol, 0.1% NH_4OH; Eluent 2: Methanol, 0.1% NH_4OH; Eluent 3: 1:1 Ethyl lactate: benzyl alcohol. This solvent selection was informed by earlier GC-FID studies which identified the key solvents detectable in the ink [1].

Ultrahigh performance liquid chromatography-photodiode array-mass spectrometry

To further identify the individual colorants, ink and dye standard samples were diluted in methanol or tetrahydrofuran (THF) to approximately 0.1%; TLC bands were scraped from the plate and shaken in approximately 0.5 mL THF. All samples were filtered through a 0.2 µm Teflon filter prior to analysis. Analysis was conducted using a Waters Acquity UHPLC system with a photodiode array detector followed by a Bruker MicrOTOF-Q II mass spectrometer. The separation was carried out on a Waters BEH-C18 column (2.1 × 50 mm, 1.7 µm particle size) with gradient elution (Solvent A: 5 mM NH_4OH in water; Solvent B: methanol. 0.0–1.0 min, 100%A; 1.0–3.0 min, linear gradient to 100%B; 3.0–4.0 min, 100% B. Flow rate 0.5 ml/min, injection volume 2 µl, column temperature 40 °C.) The mass spectrometer was operated in positive ion electrospray mode, collecting *m/z* 200–2000, and calibrated with a post-run infusion of 10 mM sodium formate.

Size exclusion chromatography

Size exclusion chromatography was conducted to test for the presence of any polymeric fraction using an Agilent 1100 model HPLC equipped with two PLgel MIXED-D columns (300 × 7.5 mm, particle size 5 µm) and a Refractive Index detector. The eluent was THF at 35 °C at a flow rate of 1.0 mL/min. Samples were diluted to 1 mg/mL, and 100 µL was injected. The system weight was calibrated with ten narrow polystyrene standards in the range 580–371,000 g/mol, dissolved in THF at 0.5 mg/mL.

Canvas tensile properties

The tensile properties of an unprimed unpainted heavyweight cotton duck 'mockup' canvas (Russell and Chapple, UK) were characterized with and without soiling with ink. The test canvas had a reasonable likeness to the painting canvas weight, with a plain weave with two adjacent warp yarns perpendicular to a single thicker weft yarn (Fig. 2B). The warp yarns (horizontal direction) were 0.363 mm in diameter with 26.8 warp ends per cm. The weft yarns (vertical direction) were 0.393 mm in diameter with 11.4 weft ends per cm. For comparison, the T01170 canvas of the Rothko painting is one piece of cotton-duck fabric with a plain weave and medium weight. The warp yarns have an average number of 17 warp ends per cm, while the weft yarn has an average number of 13 weft ends per cm [18].

The canvas was prepared by placing it over a piece of foam board (8-mm thick), stretched over the board edges, and anchored with thumbtacks to the back and front sides of the board to create adequate tension. The ink was applied to one side using a 3-inch natural-hair paint brush (the use of the plastic-foam tipped applicators used on the painting was not efficient for creating larger areas of inked sample). The brush was either lightly or heavily loaded with ink to mimic heavy and light applications on the painting. The ink was brushed out vigorously, which dried almost instantaneously after application. This process was carried out in an uncontrolled laboratory environment, using a portable extraction unit to remove solvent vapor. The room conditions (23 °C, 47–50% RH) were noted at the time of the ink application. The canvas was left to dry in a vertical position (to mimic the painting orientation) for approximately two weeks at ambient temperature and exposed to low daylight fluorescent tube light levels. The canvas was stored for the next two weeks under variable environmental conditions within the range of 35–60% RH and 17–24 °C while being shipped to the site of the tensile experiments, and stored in the dark at 23 ± 2 °C and 50 ± 5% humidity thereafter.

Rectangular specimens (5.1 × 2.5 cm) were cut from the canvas with a sharp metal die and an electric clicker press (QUALITEST™, Model SE 8) in two perpendicular canvas orientations, and then stretched uniaxially in a tensile testing frame. The average weights of a set of square canvas specimens (5.1 × 5.1 cm, 4 to 6 specimens, precision reported to ± two standard deviations) associated with none, light, and heavy ink levels (0.799 ± 0.007, 0.785 ± 0.034 and 0.956 ± 0.024 g) were measured after the ink had dried. It follows that the weight fraction of the

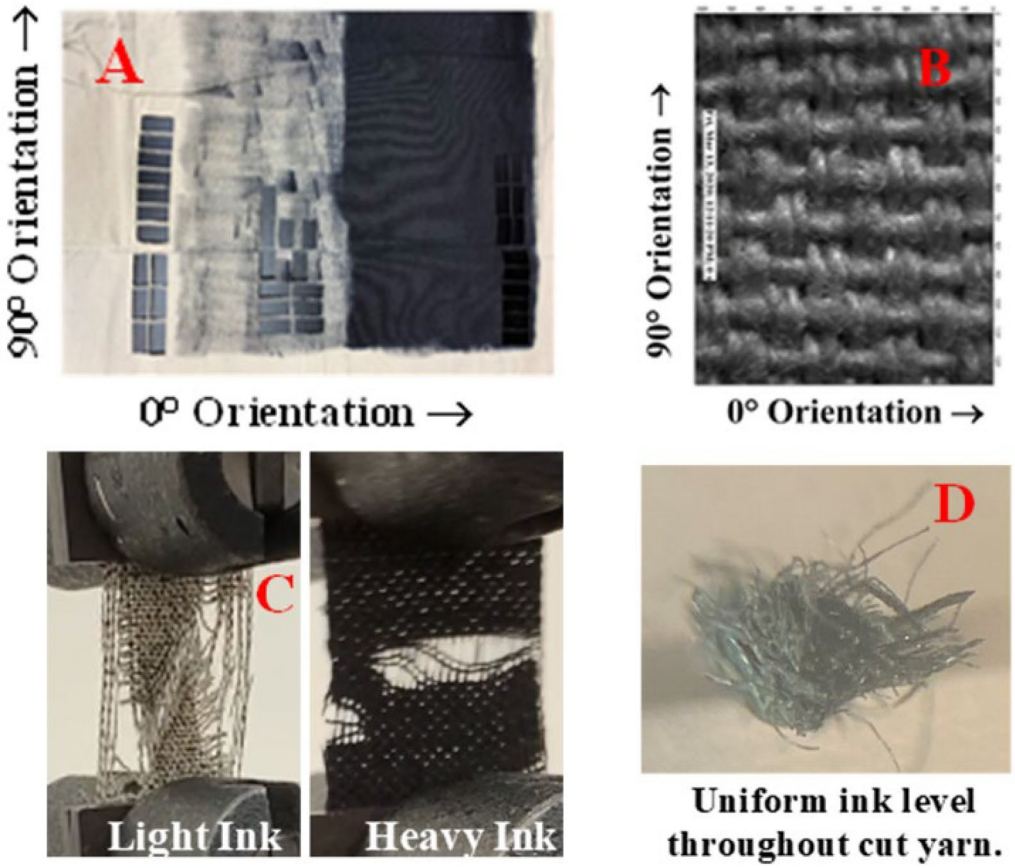

Fig. 2 **A** The large cotton duck canvas was soiled with three ink levels; rectangular specimens were cut parallel to the two perpendicular fiber orientations. **B** This plain weave canvas has two adjacent (vertical) warp yarns perpendicular to a single thicker (horizontal) weft yarn in this enlarged (microscope) image. **C** Images of two representative canvas specimens, soiled with either light or heavy ink levels, approaching their tensile break strains (90° orientation). **D** Enlarged (microscope) image of the end of a sharply cut weft yarn (0.393-mm diameter) taken from the heavy-ink canvas

residual ink colorants on the light- and heavy- soiled canvases are 0.00 ± 0.04 (not measurable) and 0.20 ± 0.04 g. Images of the specimens with either light- or heavy- ink soiling indicated similar ink levels on the front and back side even though the ink was applied to only one side of the canvas (to mimic the incident). A microscope image of a sharply cut end of one representative weft yarn (0.393-mm diameter) taken from a canvas soiled at the heavy-ink level is shown in panel (D) of Fig. 2. The ink colorants appear roughly uniformly distributed across the yarn diameter even though the ink was applied only from one side of the canvas. The ink colorants appear also to roughly uniformly coat and adhere to the surfaces of the numerous (cellulose) cotton fibers throughout the yarn interior. These visual images are intended to qualitatively show the ability of the ink to flow around the yarn perimeter and to penetrate its interior. Quantitative measurements of the ink levels around the perimeter and interior of all canvas yarns were out of scope for this study.

The data measured over an eight-month period provides a first-pass assessment of the short- and medium-term ink impact on the mechanical strength of the painting canvas support in large-strain uniaxial extensional mode. The setup and approach were guided by ASTM D5034 involving a strain-controlled servo-electric testing frame (Model 5567A, INSTRON™) operated with data acquisition software (Bluehill, version 4.06.23671, INSTRON™). The ends of the cut rectangular canvas specimen were held with pneumatic sample grips (552 kPa), and the specimen top was stretched by the upward motion of the sample grip. The tensile force was measured with a 1-kN load cell placed between the top sample grip and the horizontal crosshead bar. The dimensions of all rectangular specimens were the same (5.08 cm long, 2.54 cm wide, 0.0686 cm thick). Only the portion of the specimen between the pneumatic grips was subjected to tensile deformation, and its initial (gage) length was 2.54 cm. The tensile stretch rate

was constant (50.8 cm/min) for all specimens. All tensile properties were measured in a constant temperature/humidity laboratory (23 °C, 50% humidity). The stretching of selected specimens was video recorded to verify the absence of undesirable issues (e.g., specimen slippage in the grips; break points at the specimen/grip interface, etc.). Time-resolved measurements of the tensile force F and displacement D were recorded as the specimen is stretched. About 500 data points were commonly collected when the specimen was stretched about three cm. Subsequently, the displacement was transformed into an engineering tensile strain ε ($=D/D_0$-1) based on the displacement D and its value D_0 at the start of the tensile experiment. Similarly, the tensile force F was transformed into an engineering tensile stress σ (F/A) by dividing of the tensile force F by the specimen cross sectional area A ($W \bullet T = 1'' \bullet 0.027''$) at the start of the tensile experiment. The tensile break point of each stress/strain curve was identified as the data point with the highest tensile stress σ. Mean tensile break properties (stress $<\sigma_B>$ and strain $<\varepsilon_B>$) are reported after averaging the results of 16 replicates, where the tensile break stress is equivalent to the tensile strength. The relative precision of both mean tensile break properties is estimated to be ± 9% at the 95% confidence limit. The tensile properties were always measured on the same day the canvas was cut and the properties were measured 81 and 259 days after the canvas was soiled with ink.

Ink hansen solubility sphere

The Hansen solubility Parameters (HSP) of the ink solute were determined by first evaluating the ink solubility in 18 solvents with a range of polarity and hydrogen bonding properties. The solvents chosen for study were as follows: Acetonitrile; Ethylene Glycol n-Butyl Ether; Dibutyl Ether; Dimethyl Formamide; Dimethyl Sulfoxide; Methanol; 2-Butanone; 4-Methyl-2-pentanone; n-Butyl Acetate; n-Heptane; 1-Propanol; o-Dichlorobenzene; Tetrachloroethylene; 1,2-Propanediol; Tetrahydrofuran; Toluene; Propylene Carbonate; and Water. The individual solvent-ink samples were prepared at 5% (weight/ volume) at room temperature. The samples were mixed on an Eberbach shaker for 24 h, then removed and allowed to sit for 30 min before being visually rated on a scale of 1 (Completely soluble) to 6 (Insoluble) as per the criteria shown in Table 1. The numerical ratings were then inputted into a Dow bespoke SOLFIT program, CHEMCOMP™ Solvent Property Modeling Service [19], to obtain the HSP and radius of interaction (R values) for the solute utilizing the empirically derived Hansen's method [20–22]. These values were entered into Dow's solvent database and a RED (Relative Cohesive Energy Difference) search was conducted against the approximately 600 solvents in the database. From this search, solvents with RED < 1 were identified for potential use, which were evaluated and taken forward to the painting treatment as detailed by Ormsby et al. [1]. Note that Hansen's commercially available HSPiP (Hansen Solubility Parameters in Practice) program can carry out a similar calculation [23].

Table 1 Criteria used for evaluating solvents for the determination of the Hansen Solubility Parameters

Rating	Rating description	Explanation
1	Completely soluble	No visible solute particles
2	Almost soluble	Only a small amount of solute particles left
3	Strongly swollen	Solute swelled in size and or broken into smaller swollen particles
4	Swollen	Solute has significantly swollen in size
5	Slightly swollen	Solute shows some swelling
6	Insoluble	Solute unchanged

Results and discussion

Ink compositional analysis

While many of the analytical techniques employed provided simultaneous information on colorants, film formers and other constituents, for simplicity—and to accurately reflect the key analytical findings—the following section has been divided into ink binder, solvents, additives, and colorants.

Ink 'binder'

High-magnification observations and simple scratch tests of dried ink samples revealed that the ink was prone to brittle fracture and therefore of low molecular weight. Pyrolysis GC–MS (described below) did not reveal any fragments likely to represent a polymeric binder or any oligomeric species. Size exclusion chromatography of the THF-soluble components confirmed there was no high molecular weight component in the ink; the molecular weight distribution was multimodal, with an upper limit around 10,000 Dalton. This is similar to the distribution found for nigrosine Solvent Black 7 dye and supports the interpretation of the scratch test that no ink binder/film former is present in the formulation. A lipid fraction was detected in the GC–MS analysis (described below), which was likely to have been utilized in the formulation as an additive and/or carrier solvent to solubilize the dye.

Ink solvents & additives

The Molotow graffiti ink is a dilute, densely colored product designed to be highly staining, and hence contains a high proportion of solvent and colorant. The ink is approximately 27% solids, and the presence of ethanol

and 1-methoxy-2-propanol (propylene glycol monomethyl ether) were listed on the Safety Data sheet obtained from the manufacturer. As previously reported the carrier solvents were identified via GC-FID as a 2:1 ethanol and 1-methoxy-2-propanol blend, with other solvents (e.g., methanol, 2-butanone and ethyl acetate) present at trace (< 1%) amounts [1].

GC–MS was conducted on an acetonitrile solution of the ink; acetonitrile was chosen because it would be nonreactive in the injection port and has similar solvation characteristics as the carrier solvents. While the larger dye molecules may not be fully soluble, acetonitrile should dissolve the smaller molecules amenable to GC. Analysis of the ink confirmed the presence of the solvents previously identified, as well as a lipid fraction containing octanoic, decanoic, and oleic acids, and their ethyl esters (Fig. 3). Glycerin monopalmitate and glycerin monostearate were also detected. Fatty acids and esters may be present to aid in wetting the substrate, or to inhibit drying of the marker tip. Ethyl oleate is known as a solvent for fat-soluble dyes such as Solvent Black 7 [24], and/or additive for inks [25]. Diphenylamine was also detected and is likely to be a fragment or constituent of the nigrosine dye, since it was also observed in the pyrolysis GC–MS of the Solvent Black 7 dye standards (see below).

Ink colorants

Previously reported elemental and microscopic analysis suggested that the colorant is largely carbon-based with the appearance of lamp black, with trace amounts of sulfur, sodium, silicon, copper, aluminum, chlorine and iron [1]. However, subsequent work demonstrated that the colorant is entirely mobile with certain eluents in TLC, showing that the colored species are soluble and thus do not include carbon black or other inorganic pigments. The iron and copper elements were however detected (see ICP-MS below) and originate from the specific dyes used. The ink bottle label states that the color is signal black (RAL 9004), which does not provide compositional information on the likely colorants used, though the additional description of "synthetic bitumen" suggests that the colorant may be of petro-organic origin. Further analysis using thin layer chromatography, liquid chromatography, infrared spectroscopy, pyrolysis-GC, and mass

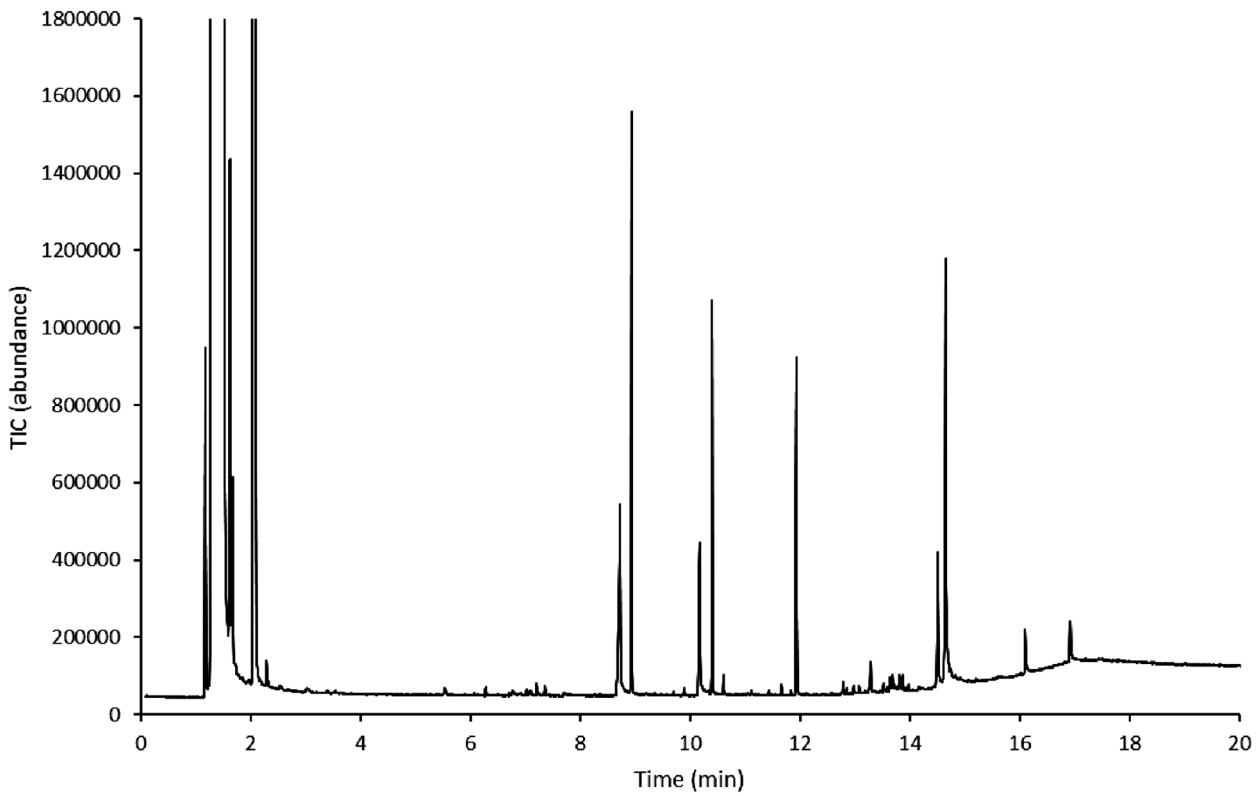

Fig. 3 GC–MS total ion chromatogram of Molotow ink diluted in acetonitrile. Peaks were identified as: ethanol (1.28 min); 2-butanone (1.63 min); α-Propylene glycol monomethyl ether (2.09 min); Octanoic acid (8.74 min); ethyl octanoate (8.94 min); n-Decanoic acid (10.18 min); ethyl decanoate (10.41 min); Diphenylamine (11.94 min); Oleic Acid (14.51 min); Ethyl Oleate (14.66 min); glycerin monopalmitate (16.11 min); glycerin monostearate (16.92 min)

spectrometry shown in the subsequent sections confirm the colorants include the fat-soluble nigrosine-type (phenazine) dye Solvent Black 7 [26] and the metal-complex solvent-soluble phthalocyanine-type Solvent Blue 70 [27] dye, the latter of which was listed on the SDS sheet obtained in 2015. Details of these analyses are as follows.

FTIR Absorption bands (at 3300, 1589, 1489, 1445, 1025, 1002, 745, 693 cm^{-1}) in FTIR spectroscopic analysis of dried ink suggested the presence of an aniline-black type nigrosine dye (based on comparison to in-house databases and published spectra [28]). This was further explored using FTIR spectroscopy by obtaining samples of two nigrosine-based solvent dyes (Solvent Black 5 and Solvent Black 7) in addition to the phthalocyanine-based dye Solvent Blue 70. Spectra of Solvent Black 5 and Solvent Blue 70 were not ideal matches for the FTIR spectrum of the dried ink. Solvent Black 7, however, shows several absorption bands which closely match the spectrum of the dried ink. Of course, the spectrum of dried ink will represent the spectral combination of all nonvolatile components; indeed, CH and carbonyl stretching bands attributable to the fatty acids and esters observed by GC–MS are visible in the ink spectrum and not the dyes. The spectra of Solvent Black 7, Solvent Blue 70, and the dried ink are shown in Fig. 4. The chemical structures of Solvent Black 7 (I) and Solvent Blue 70 (II) are shown in Fig. 5; note that Solvent Black 7 consists of multiple chemical structures in the pattern depicted in the figure, it is not a single molecular species. The presence of Solvent Black 7 was also confirmed by pyrolysis GC–MS as outlined below.

TLC Numerous solvents were explored with three key eluents (listed in the *Experimental* section) providing useful insight into the colorant composition. Using Eluent 1, all the colorant within the ink traveled with the solvent front. This demonstrates that the colorants are all organic dyes soluble in this solvent and thus eliminated the possibility of inorganic pigments and carbon black from the formulation. Using Eluent 2, several colored bands in the ink are resolved, as follows: blue, $R_f = 1$; light purple, $R_f = 0.95$; pink, $R_f = 0.24$; plus a black spot remaining immobile. Under the same conditions, Solvent Blue 70 produced a matching blue band at the solvent front; Solvent Black 7 produced matching-colored bands at $R_f = 0.95$ and $R_f = 0.24$; and Solvent Black 5 produced deep purple bands at $R_f = 0.96$ and 0.92 which did not match any of the bands from the ink.

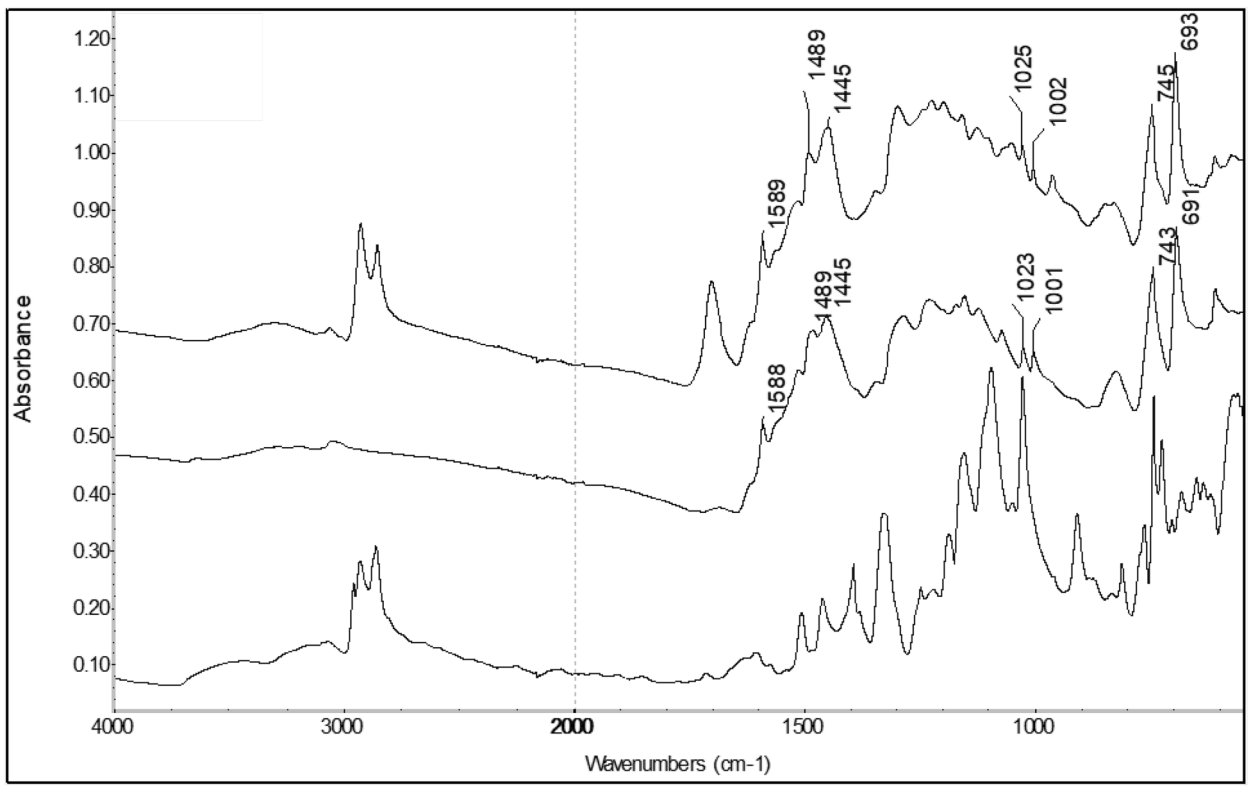

Fig. 4 FTIR spectra of dried graffiti ink (top trace), Solvent Black 7 (middle trace), and Solvent Blue 70 (bottom trace); spectra shifted vertically for clarity

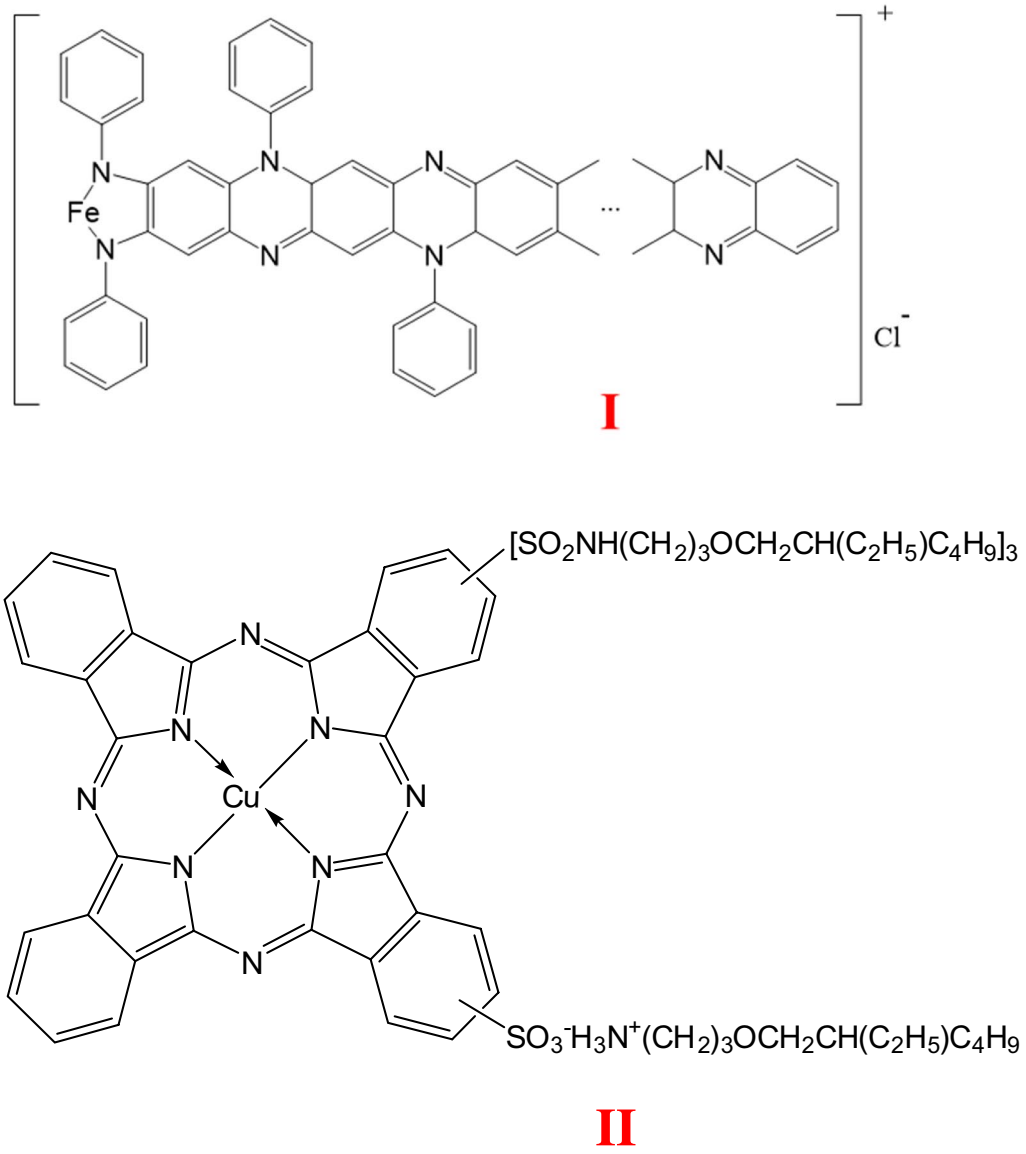

Fig. 5 Chemical structures of proposed ink components Solvent Black 7 (I) and Solvent Blue 70 (II)

This suggests that the ink colorants include Solvent Blue 70 and Solvent Black 7 but not Solvent Black 5 which was therefore not further considered.

Eluent 3 was chosen because it represented the solvent combination chosen based on the Hansen Solubility Parameter study for removing the ink material during the conservation treatment of the artwork. Using this eluent, most of the colorant eluted with the solvent front, with a broad light purple band at R_f 0.35. This confirmed that all the colorants were soluble in this solvent, which supports the use of this solvent blend for the removal of the ink from the painting[1].

ICP-MS Analysis of the ink by ICP-MS revealed the presence of 260 ± 45 ppm iron, and 215 ± 30 ppm copper. This is consistent with the presence of Solvent Black 7 (synthesized by heating nitrobenzene, aniline, and aniline hydrochloride in the presence of an iron catalyst) and Solvent Blue 70 (a copper phthalocyanine). No other metals > 1 ppm were detected.

Pyrolysis GC–MS The major peaks in Solvent Black 7 (benzene, benzene isocyanate, aniline, biphenyl, diphenylamine, and dibenzopyrrole) are all found in the pyrogram of the ink. Other major peaks found in the pyrolysis of the ink include several of the formulation components identified in the liquid injection-GC–MS data (palmitic, stearic and oleic acids, methyl oleate and ethyl oleate). The pyrogram for Solvent Blue 70 exhibits many peaks which are not present in the ink pyrogram, including fragments suggesting ethylhexyl or isooctyl chains, and 2-ethylhexyloxypropylamine; the source for the lab standard used here compounds the dye 1:1 with 2-ethylhexyloxypropylamine, which explains these pyrolysis products. Other suppliers may well select other compounding species, so the absence of these peaks in the ink pyrogram does not exclude the presence of Solvent Blue 70. No pyrolysis products from the phthalocyanine moiety itself were detected in the pyrogram of Solvent Blue 70, presumably due to its highly conjugated structure; hence pyrolysis GC–MS could not confirm its presence in the ink. The pyrolysis GC–MS total ion chromatograms are given in the Additional file 1.

UHPLC-PDA-MS Using Eluent 2, the blue TLC spot from the graffiti ink with $Rf = 1$ was scraped from the plate and redissolved in methanol, alongside the corresponding spot from Solvent Blue 70. Analysis of these spots by UHPLC-PDA (using 400–500 nm, the visible wavelengths in the PDA range, Fig. 6) shows several colored peaks detected, with good correlation between the samples. While these peaks did not produce meaningful ions by electrospray ionization, the UV–Vis spectra of each of

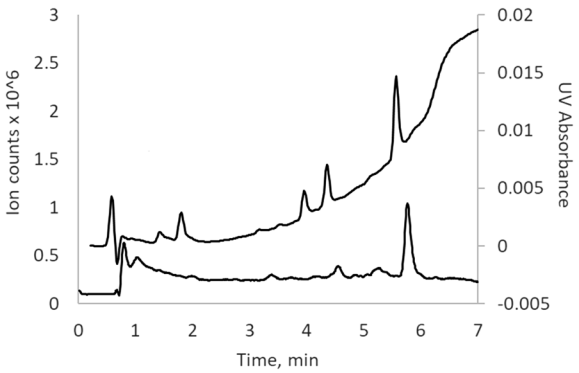

Fig. 7 UHPLC-PDA-MS chromatograms of purple TLC band from the ink, showing the absorbance trace (400–500 nm, top) and the positive electrospray-MS base peak chromatogram (bottom)

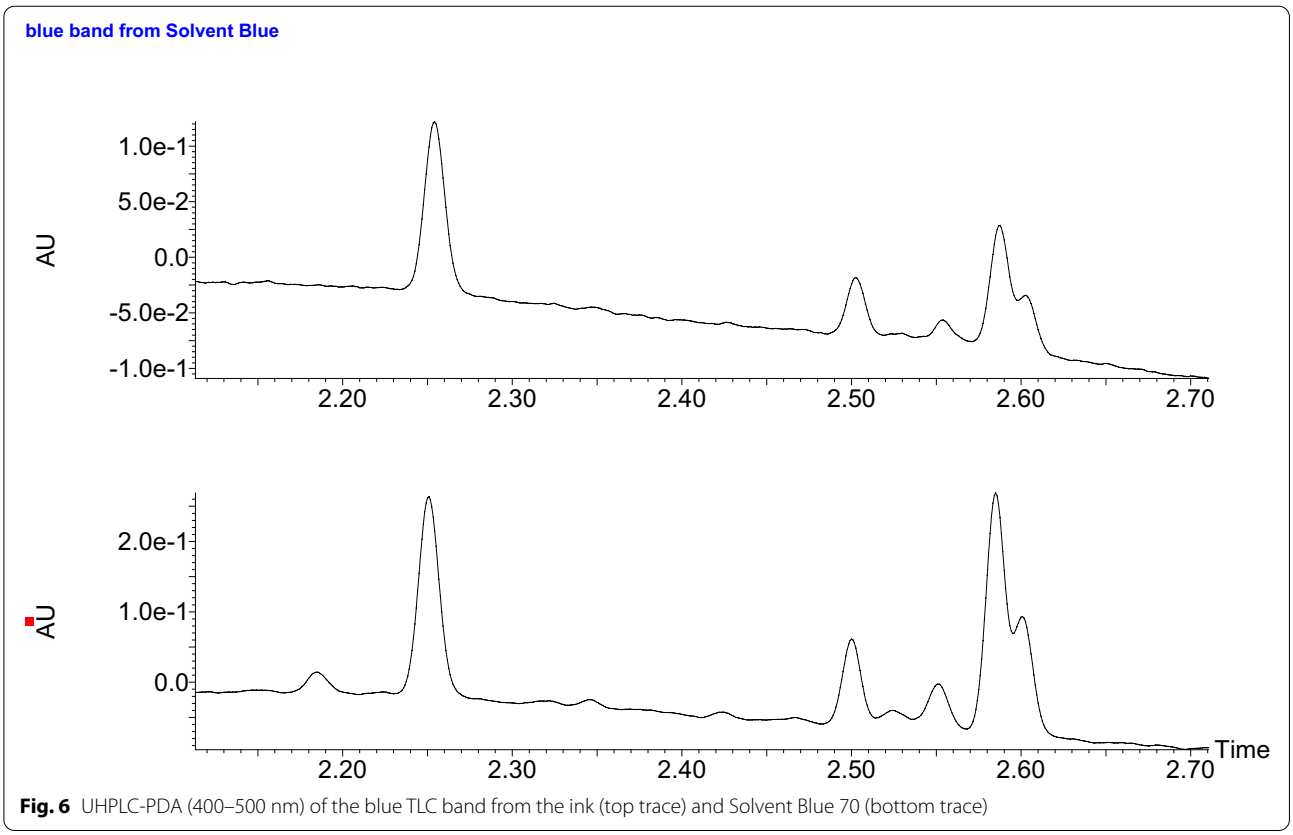

Fig. 6 UHPLC-PDA (400–500 nm) of the blue TLC band from the ink (top trace) and Solvent Blue 70 (bottom trace)

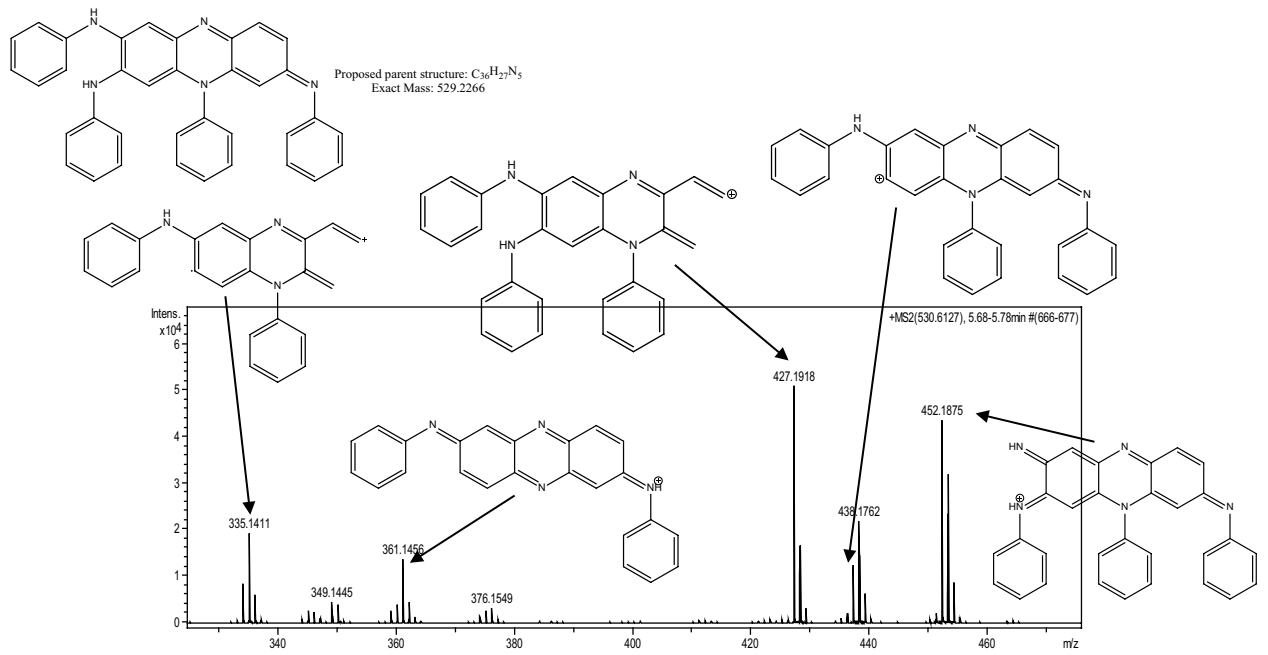

Fig. 8 MS–MS spectrum of peak eluting at 5.6 min in the absorbance chromatogram of Fig. 7 with parent ion *m/z* 530.2332, showing proposed fragment structures

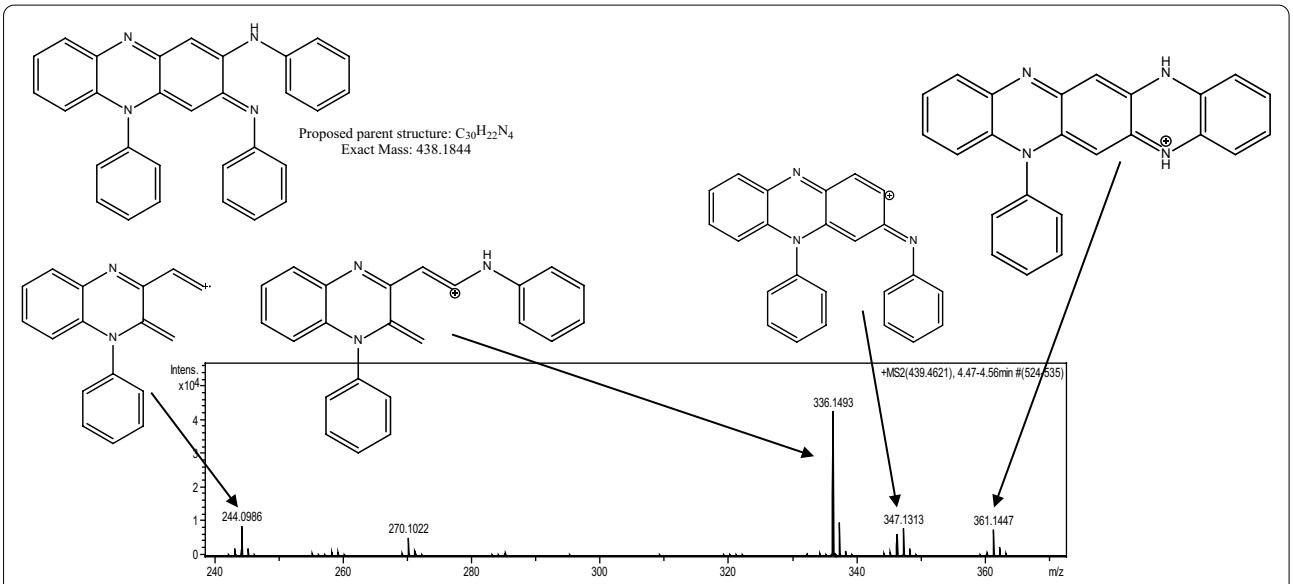

Fig. 9 MS–MS spectrum of peak eluting at 4.4 min in the absorbance chromatogram of Fig. 7 with parent ion *m/z* 439.1915, showing proposed fragment structures

the major chromatographic peaks provides a good match between the two chromatograms. These spectra are given in the Additional file 1 This evidence supports the presence of Solvent Blue 70 in the ink.

Similarly, the purple TLC band at $Rf = 0.95$ of the ink was scraped from the plate and redissolved, and analyzed by UHPLC-PDA-MS. Four peaks with an absorbance in the visible spectrum (400–500 nm) are detected in this band and gave a detectable signal by electrospray-MS

in positive mode; see Fig. 7. The most intense of these, eluting at 5.6 min in the absorbance chromatogram, produceds a protonated ion at *m/z* 530.2332. The proposed structure, shown in Fig. 8 has the formula $C_{36}H_{27}N_5$ and a protonated mass of 530.2345 Da (a difference from the observed ion of + 0.0013 Da, or + 2.45 ppm). By MS–MS the two most prominent product ions were *m/z* 427.1918 and 452.1875 (neutral losses correlating to C_6H_6 and C_7H_5N) which are consistent with the nigrosine structure of Solvent Black 7. Figure 8 shows the MS–MS spectrum of this parent ion, with proposed structures for the fragments.

The next most prominent peak in the PDA chromatogram eluted at 4.4 min with a MS ion at *m/z* 439.1915; the proposed structure shown in Fig. 9 has the formula $C_{30}H_{22}N_4$, and a protonated mass of 439.1923 Da (a difference from the observed ion of + 0.0008 Da, or + 1.82 ppm). The MS–MS spectrum of this parent ion is shown in Fig. 9 along with the proposed fragment structures; notably the species exhibits two prominent MS–MS product ions showing neutral losses of C_6H_6 and C_7H_5N, suggesting this is also a nigrosine species.

The remaining two bands which produced signal in both the PDA and MS data elute at 1.8 and 3.95 min, with molecular ions at *m/z* 364.1440 and 455.1844, respectively. These parent molecules each fragment with the characteristic nigrosine neutral losses noted above and produce an ion with a neutral loss correlating to CO. The parent structures of these peaks have not been elucidated, and may represent oxidized forms or other derivatives of the nigrosine dye.

MALDI-TOF MS An overlay of the MALDI spectra of the dried ink and Solvent Black 7 is shown in Fig. 10. Many of the ions are identical, although the relative intensities are not always consistent. This may be due to variability among suppliers of Solvent Black 7, and/or additional components present in the commercial ink. For many of the observed ions, such as that at *m/z* 800, the only significant ion produced on further fragmentation by MS–MS is a neutral loss of 77 Dalton, consistent with the nigrosine dye structure. It is beyond the scope of this work to elucidate each of the ions observed in the MALDI-MS spectrum, in this case the spectral similarity was taken as supporting evidence for the presence of Solvent Black 7.

Ink solubility and HSP value determination

Determining the solvent blend used on the painting has been described in detail elsewhere [1]. This section summarizes the determined dried ink HSP values and solvent class recommendations resulting from the regression of the solubility data that supported the final solvent blend selection. The HSP values obtained for the ink were: Hansen Dispersion Parameter = 17.94 (J/

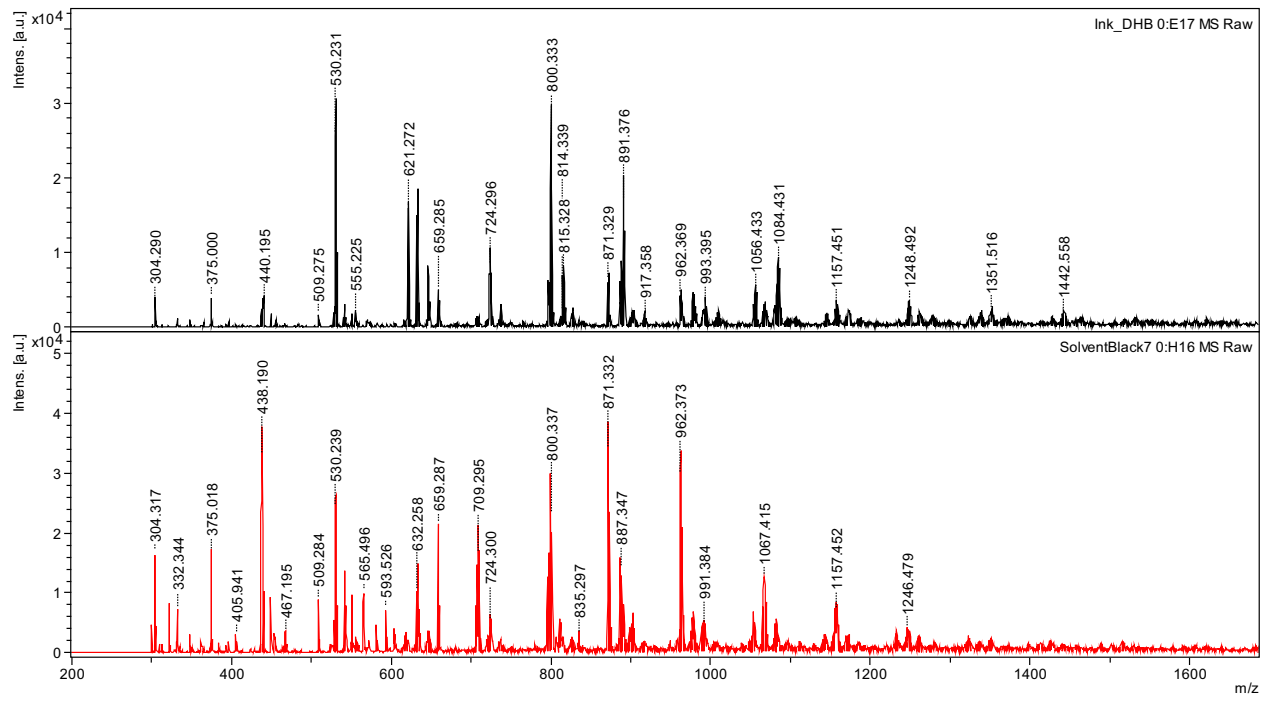

Fig. 10 MALDI mass spectra of graffiti ink (top) and Solvent Black 7 (bottom). Many of the ions are identical, although the relative ratios vary somewhat

cc)$^{1/2}$, Hansen Polar Parameter = 7.91 (J/cc)$^{1/2}$, Hansen Hydrogen Bonding Parameter = 12.01 (J/cc)^{½}, and Radius of Interaction = 10.6 (J/cc) $^{1/2.}$ The general classes of solvents predicted to have high solubility for the ink included alcohols, ethers, esters, and ketones. A second set of calculations were executed on the solubility of aged alkyd as a simplified surrogate for the painting. From over 600 solvents, a group of 16 solvents that had high ink solubility predictions (i.e., low RED values) coupled with low aged alkyd solubility predictions (i.e., high RED values) across a range of solvent classes were chosen, with additional restrictions applied with regards to health and safety considerations. These solvents were the following: methanol, ethanol, benzyl alcohol, DOWANOL PPH Glycol Ether, DOWANOL EPH Glycol Ether, DOWANOL DiPPh tech, methyl carbitol, ethyl lactate, n-butyl alcohol, isobutyl alcohol, hexylene glycol, acetone, n-propyl alcohol, DMSO, propylene glycol, ethylene glycol diethyl ether. The process outlined above saved considerable time by avoiding the need to generate a Teas diagram for the ink. Teas diagrams are used within art conservation to map the solubility characteristics of resins and polymers through their dispersion, polar and hydrogen bonding intermolecular forces [29]. The ink solubility characterization, modeling predictions and early experimental results guided the rigorous process of selecting the most effective cleaning system which included exploration of over 75 systems, evaluated across a range of substrates [1–3] prior to beginning the ink removal process on the painting.

Ink legacy and the canvas support

Cotton duck canvas is valued for its mechanical flexibility, and high mechanical strength, which are critical for (1) supporting the weight of large paintings, (2) withstanding biaxial stretching when placed in a jig (canvas

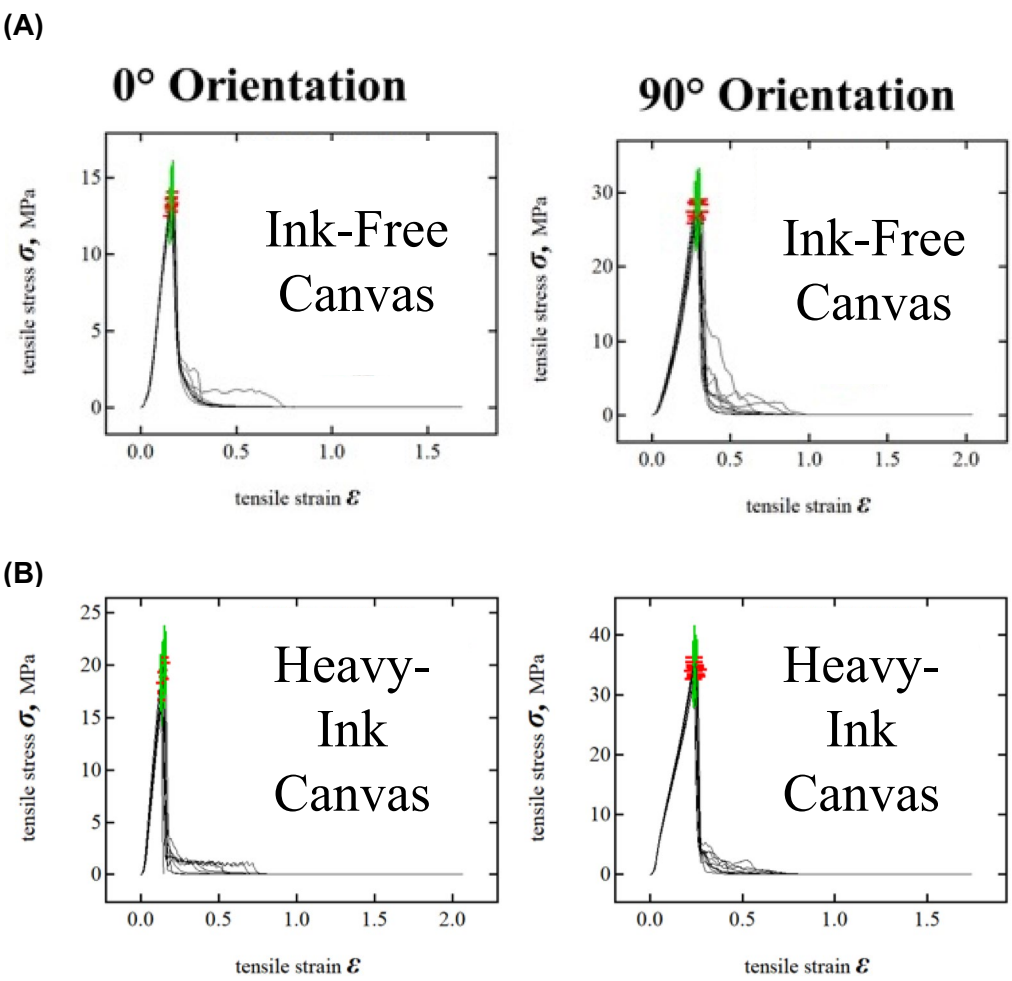

Fig. 11 **A** Dependency of the tensile stress (σ) on the applied strain (ε) for two orientations of the ink-free canvas. **B** Dependency of the tensile stress on the applied strain for two orientations of the heavy-ink canvas

corners represent the high-stress site of most mechanical failures), and (3) withstanding unwanted/unexpected/accidental large-strain deformations. End-use mechanical properties of canvases often involve their strengths in uniaxial extension (tensile), biaxial extension, bending (flexural), and tearing deformations. A focus solely on uniaxial extension (tensile) deformation, as done here, only provides one key metric of performance, and has often been employed in painting conservation research [30].

A cotton duck canvas is a two-dimensional plain-weave fabric based on cotton yarn [31]. The yarn contains multiple thin fibers of cotton after the fibers have been collectively spun, twisted, and stretched in a spinning process to a target diameter and strength, and the cotton fibers are seldom surface coated with a sizing. The resulting mechanical properties are often a convolution of the mechanical properties of the thin cotton fibers and thicker cotton-spun yarns, as well as, the weave design, yarn diameter, fabric count, and yarn frictional properties [32–37].

As described in the "Experimental" section, tensile stress/strain curves were measured on the mockup for two perpendicular canvas orientations (0 and 90°) in domains associated with three levels of ink (e.g., none, light, heavy). Typical data for two contrasting ink levels are shown on linear axes in panels (A) and (B) of Fig. 11. Each continuous curve is composed of about 500 straight-line segments connecting adjacent data points. Key features of each curve are: (1) the monotonic rise of stress as strain increases, and (2) the maximum stress when the canvas breaks. A well-defined break point (e.g., stress σ_B and strain ε_B) is also evident in each curve and the superposition of the ten replicate curves, prior to the break point, is very good. The weave fibers parallel to the testing-frame stretch direction are expected to dominate the tensile properties. Consequently, data associated the 90° orientation of the cut canvas are expected to be dominated by the thinner higher-thread-count warp fibers.

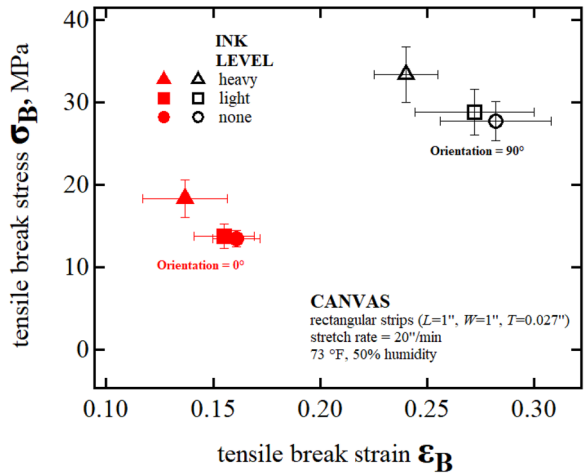

Fig. 12 Average tensile break properties measured for two canvas orientations and three ink levels

The average break point data, measured for either 81 days or 259 days after ink soiling, are summarized in Table 2 and illustrated in Fig. 12. These averages are based on 16 replicates and the precision is reported as ± 2 standard deviations. (For reference, break stresses (27.7 ± 2.4 MPa [warp], 13.4 ± 1.0 MPa [weft]) measured here for the ink-free canvas well approximate results (32.5 ± 2.0 MPa [warp], 30.8 ± 3.2 MPa [weft]) reported elsewhere [31] for a similar hard-texture duck canvas (number duck 12, 11.6 ± 0.5 oz/yard^2, thread count per

Table 2 Average canvas tensile break properties for two canvas orientations and three ink levels

Canvas Orientation	Ink Level	Break Strain $<\varepsilon_B>$	Break stress $<\sigma_B>$ [MPa]	Time since ink application (days)
0° weft	none	0.161 ± 0.011	13.4 ± 1.0	81
0°	none	0.149 ± 0.014	14.3 ± 1.6	259
0°	light	0.155 ± 0.014	13.7 ± 1.5	81
0°	light	0.137 ± 0.011	14.0 ± 1.5	259
0°	heavy	0.137 ± 0.020	18.3 ± 2.3	81
0°	heavy	0.127 ± 0.014	18.5 ± 1.3	259
90° warp	none	0.282 ± 0.020	27.7 ± 2.4	81
90°	none	0.280 ± 0.026	29.2 ± 2.5	259
90°	light	0.272 ± 0.028	28.8 ± 2.8	81
90°	light	0.273 ± 0.037	30.2 ± 2.9	259
90°	heavy	0.240 ± 0.015	33.3 ± 3.4	81
90°	heavy	0.244 ± 0.031	34.3 ± 2.8	259

cm 22 ± 2 [warp] and 14 ± 0.8 [weft]).) Break strains (and stresses) for the 90° canvas orientation (warp fibers) were found to be around twice (e.g., 27.7/13.4 = 2.1) those of the 0° orientation, for any given ink level. This anisotropy is commonly reported elsewhere [31] for lower-density (< 19 oz/yard^2) cotton duck canvases and in this case, the mockup canvas 90° orientation has about twice the thread count (ratio 68/28 = 2.4) contributing to the tensile properties (see panel B of Fig. 2). Weaker dependences were found for the break properties with respect to the ink level. The average break strain $<\varepsilon_B>$ decreased by about 15% for the weft and warp fibers as the ink level increased. In contrast, the break stress $<\sigma_B>$ increases by about 37% for the weft fibers and 20% for the warp fibers as the ink level rises. These results imply the ink soiling appears to make the mockup canvas more brittle as the level of ink applied increased.

Interpretation of this data ideally requires additional information about the chemical and physical structure of the cellulose in the mockup canvas cotton fibers, the penetration depth of the ink into the cotton fibers, the yarn spun from these fibers, and tensile strength data for individual ink-soiled cotton fibers and ink-soiled yarn. Nevertheless, the ink solvents (e.g., primarily ethanol and 1-methoxy-2-propanol) are not expected to strongly swell or chemically react with the cellulose fibers at room temperature in the brief time (seconds to minutes) available for the ink to dry. Ethanol, for example, is reported [38] to need much longer times (hours) to fully swell semi-crystalline cellulose fibers. The slow swelling rate is due to the crystals acting as physical crosslinks. As a result, the ink colorants are most likely excluded from the painting fiber interiors, and the inherent mechanical properties of the cotton fibers preserved.

The role of these colorants on the canvas tensile properties is suggested by the two contrasting images of canvas specimens in Fig. 2 (panel C). The images were taken just before the canvas specimens reached their tensile break point. The higher tensile break stress σ_B for the heavy-ink specimen arises from its higher number of vertical (warp) yarns resisting the deformation at the break point. The dried ink appears to enhance the adhesion between the canvas yarns, so they break collectively. It follows that higher colorant levels should elevate the break stress σ_B as observed.

The argument for the reduced break strain with increasing ink levels is also centered around the number of yarns breaking simultaneously. It is assumed that the strain associated with the break point of a set of yarns is initiated when the strain exceeds the break strain of the lowest-break-strain yarn. Once the first yarn of a set of yarns breaks, the others will rapidly follow. A distribution of break strains must exist for each specimen regardless of the ink level since the peak in the stress/strain curve at the break point has a finite width (e.g., see panels A and B of Fig. 2). The probability of a lower break strain yarn in the set of simultaneously breaking yarns rises when the number of yarns in the set increases. These results for the ink-soiled mockup canvas are similar to those reported elsewhere when textile materials have been coated on either one or both sides, and sometimes with multiple layers [30]. The coatings make the fabric more rigid when it fills the fabric voids between the yarns and cements the fabric warp/weft yarns into a single unit. The coating material also restricts the rotation between the yarns when the fabric is stretched. In that sense, the applied ink appears to have performed similarly to, for example, the application of a glue-based sizing onto canvas fabrics commonly practiced by Rothko and other artists for centuries.

The mechanical properties of the cotton duck canvas arise primarily from use of cellulose from cotton linters. The cellulose (type I) in these linters is a semicrystalline linear-chain polysaccharide known for its high-purity (> 98%), high crystallinity (73%), and high degree of polymerization (9,000 to 15,000) [39, 40]. Ideal cellulose chains are 1,4-linked condensation products of β-D-glucopyranose monomers ($C_6H_{12}O_6$, 180.15588 g/mol). Key chemical reactions often applied to cellulose involve the grafting of side chains to the backbone in an aqueous medium under strongly basic conditions [40], or a depolymerization of the backbone to monads in an aqueous medium under strongly acidic conditions and/or in the presence of oxygen [41]. All these types of reactions are usually accelerated with use of elevated temperatures. As a result, minimal chemical reactions are expected to occur between the ink components and the canvas cotton fibers since (1) the ink contains no strong acids or bases, (2) the ink solvent is nonaqueous, (3) the ink solvent evaporates in minutes, and (4) the ink/canvas temperature was not elevated. Moreover, any grafting of side chains to the cellulose fibers if present and if grafted under basic conditions should have a minimal impact on the canvas mechanical properties since the grafting process usually preserves the cellulose degree of polymerization.

Nevertheless, there is an inherent concern pertaining to the possible presence of trace amounts of residual acid in the canvas from the ink that may slowly cause depolymerization of the cellulose backbones before and after the ink dries. Similarly, there is potential concern that the oxygen and moisture in the air surrounding the canvas may independently cause a slow depolymerization, or that synergy between the two mechanisms may accelerate the depolymerization, which would require further assessment using a range of accelerated ageing

regimes. This is to be balanced however with knowledge of the whole painting structure (and how this also affects mechanical properties) and the protective effect of past and current preservation strategies.

The tensile strength of the canvas is expected to be strongly dependent on the cellulose degree of polymerization and is thus used here to provide a sensitive first-pass relative metric of any depolymerization. The insensitivity of the tensile strength data over a six-month study for three ink levels (none, light, heavy) summarized in Table 2 is encouraging for the stability of the painting. Nevertheless, there is insufficient tensile data at this point to reliably extrapolate such results to the anticipated painting lifetime. Nevertheless, the conserved painting, with much lower ink levels, has now been on display for over 8 years without visually exhibiting any changes to mechanical properties and will of course continue to be monitored on an ongoing basis.

Conclusions

The thorough characterization of an unknown ink material used in this shocking incident identified the specific solvents, colorants, and additives of the formulated product for the first time, through a combination of complimentary, relatively sophisticated analytical techniques which may prove beneficial to the analytical study of other novel and hitherto uncharacterized materials. This ink had not been the subject of research in the heritage field and differs in significant ways to the spray paints more frequently studied within a graffiti art context. The research carried out within the period of the conservation treatment naturally focused on the ink solvents and solubility to successfully inform the ink removal process. Early ink characterization efforts were somewhat hampered by the proprietary nature of the product, unfamiliarity with graffiti ink materials and limited analytical instrumentation suited to the elucidation of synthetic dyes. Since the project ended, iterative analytical investigations using a range of separation, spectroscopy and mass spectrometry techniques have confirmed the absence of any polymeric film forming component, the use of specific solvent-soluble dyes (Solvent Black 7 and Solvent Blue 70) and polar solvents, which align with the aims of a contemporary graffiti product designed for enhanced and permanent staining.

This information directly supports the future preservation of Black on Maroon (T01170) through exploring the risks associated with ink residues remaining within the paint layers and the canvas support. This information will more broadly support other conservation 'cleaning' treatments involving the removal of compositionally similar graffiti inks where desirable, and contributes to knowledge on the tensile properties of cotton duck artist's canvas. The ink appears to act primarily as an adhesive between adjacent canvas yarns and between the cotton fibers within the yarns much in the same way as a sizing layer. Collectively, this enhanced adhesion slightly embrittled the mockup canvas (e.g., elevated the tensile strength by 20 to 40% and reduced the tensile break strain by 15% under experimental conditions) for the highest levels of applied ink studied which is far more varied (and mostly lighter) within the painting structure itself. Extrapolating this information to the 60 + year old, rabbit skin glue-sized, multi-layered work of art with an uneven ink application and penetration is naturally difficult, however, these investigations have enabled an essentially complete understanding of the ink used and informed that the residues remaining within the paint and canvas have had a minimal impact on mechanical strength over the short- to medium- term. Further evaluation of aged samples under varying conditions may help to inform any longer-term implications.

It is the case that this ink material and the context of its use are (hopefully) unique, however the exploration of this single material adds to the growing body of technical literature on graffiti (and graffiti art) materials. The solubility parameter work was novel at the time of the treatment, and one of the solvents used (ethyl lactate) derived from the HSP work is now more widely used in the context of sustainability in conservation. Finally, it is hoped that the suite of instrumentation and approaches used to explore and specifically identify the ink constituents and properties may act as a useful guide where unknown materials have been used to either damage, augment, or create works of art.

Abbreviations

ATR: Attenuated total reflectance; FTIR: Fourier Transform Infrared (Spectroscopy); GC-FID: Gas chromatography-flame ionization detection; GC–MS: Gas chromatography-mass spectrometry; HPLC: High performance liquid chromatography; HSP: Hansen solubility parameter; ICP-MS: Inductively Coupled Plasma- Mass Spectrometry; IR: Infrared; MALDI-TOF–MS: Matrix Assisted Laser Desorption/Ionization-Time of Flight Mass Spectrometry; PDA: Photodiode array; RED: Relative cohesive energy difference; SEC: Size exclusion chromatography; THF: Tetrahydrofuran; TLC: Thin layer chromatography; UHPLC: Ultra-high performance liquid chromatography; UV: Ultraviolet.

Supplementary Information

The online version contains supplementary material available at https://doi.org/10.1186/s40494-022-00770-x.

Additional file 1: **Figure S1.** Pyrolysis GC-MS of dried ink. **Figure S2.** Pyrolysis GC-MS of Solvent Black 7. **Figure S3.** Pyrolysis GC-MS of solvent blue 70. **Figure S4.** UV-Vis spectrum (300-500 nm) of peak eluting at 2.25 min from solvent Blue 70 (top) and ink (bottom). **Figure S5.** UV-Vis spectrum (300-500 nm) of peak eluting at 2.50 min from solvent Blue 70 (top) and ink (bottom). **Figure S6.** UV-Vis spectrum (300-500 nm) of peak eluting at 2.55 min from solvent Blue 70 (top) and ink (bottom). **Figure S7.** UV-Vis spectrum (300-500 nm) of peak eluting at 2.59 min from solvent

Blue 70 (top) and ink (bottom). **Figure S8.** UV-Vis spectrum (300-500 nm) of peak eluting at 2.60 min from solvent Blue 70 (top) and ink (bottom).

Acknowledgements
Brian Nickless and Kayla Galbraith (The Dow Chemical Company) executed the tensile experiments. Felipe Donate (The Dow Chemical Company) supported the Ink solubility and HSP value determination. Irina Peshenko, Elizabeth Snow, and Richard Cooper, (The Dow Chemical Company) provided additional analytical support for GPC, ICP-MS, and MALDI-TOF analyses. Bronwyn Ormsby would like to thank and acknowledge all Tate colleagues, Christopher Rothko, Jaap Boon (Jaap Boon Enterprises) and wider group of collaborators and colleagues who generously contributed to the Rothko Conservation Project (2012-2014), with particular thanks to her fellow Project team members Rachel Barker (former Painting Conservator, Tate) and Patricia Smithen (former Head of Conservation, Programme, Tate).

Author contributions
STW led the collection and analysis of data regarding the ink composition and produced the first draft of the manuscript. RLS led the tensile testing of the ink-treated canvas. BAO led the scientific aspects of the Tate conservation project including several preliminary collaborative analytical studies on the ink material, produced the mockup canvas used for tensile testing, and helped devise the research questions addressed in this paper. MHK led the determination of the Hansen Solubility Parameters of the ink. All authors contributed to, read, edited and approved the final manuscript.

Authors' information
Dr. Bronwyn Ormsby is Principal Conservation Scientist at Tate, London, UK and leads the Conservation Science and Preventive Conservation section of Tate's Conservation Department. Bronwyn was the Tate scientist attached to the Rothko Conservation Project (2012–2014). Dr. Scott Wills is a Research Scientist in the Analytical Science department at Dow, USA, specializing in liquid chromatography, gas chromatography, and mass spectrometry. Dr. Melinda Keefe is a R&D Director at Dow, USA, leading a team of scientists and engineers that drive new product and bespoke automated system development. Melinda has leveraged Dow's technical expertise to technical challenges in the field of art conservation science for many years, including the Rothko Conservation Project. Dr. Robert Sammler is a material scientist with publications, presentations, and patents in many diverse topics (thermoplastics, thermosets, cellulosic ethers, low-K dielectrics, composites, low-Tg inorganic glasses, pharmaceutical excipients, suspensions, granular materials, self-assembly, reactive extrusions, interfacial tension, and phase separation).

Funding
The Tate 2012–14 Rothko Conservation project (https://www.tate.org.uk/about-us/projects/rothko-conservation-project) was funded by Tate Patrons and the Tate Fund. Any work carried out since that time has been internally (core) funded by The Dow Chemical Company and Tate.

Availability of data and materials
Data is available within this manuscript and upon request.

Declarations

Competing interests
The authors declare no competing interests.

Author details
[1]The Dow Chemical Company, 400 Arcola Road, Collegeville, PA 19426, USA. [2]Conservation Department, Tate Britain, Millbank, Pimlico, London, UK. [3]The Dow Chemical Company, 1712 Building, Midland, MI 48674, USA. [4]The Dow Chemical Company (retired), 1702 Building, Midland, MI 48674, USA.

Received: 12 April 2022 Accepted: 15 August 2022
Published online: 10 September 2022

References

1. Ormsby BA, Barker R, Keefe MH, Tucker C, Donate F, Smithen P. The removal of graffiti ink from Mark Rothko's Untitled (Black on Maroon), 1958. A collaborative approach. In Brigland J, editor. *Preprint of ICOM-CC 17th Triennial Conference, Melbourne, Australia, September 17–19, 2014*. Paris, France: The International Council of Museums; 2014. pp 1007–1014. ISBN 978-92-9012-410-8
2. Barker R, Ormsby BA, Smithen P. The construction of a representative sample for Mark Rothko's Untitled (Black on Maroon) (1958). In Brigland J, editor. *Preprint of ICOM-CC 17th Triennial Conference, Melbourne, Australia, September 17–19, 2014*. Paris, France: The International Council of Museums; 2014. pp 1302- 1309. ISBN 978–92–9012–410–8.
3. Ormsby B, Barker R, Keefe MH, Donate F. Reflections on the Diagnostic Tools and Methodologies Used to Support the Conservation Treatment of Mark Rothko's Painting 'Black on Maroon', 1958. CON_360. Accessed 7 August 2022.
4. Carlyle L, Boon JJ, Bustin M, Smithen P. The substance of things. London: Tate Modern; 2008.
5. Molotow Masterpiece™ Coversall Cocktail Graffiti Ink Product Information Web Page. https://shop.molotow.com/en/marker-refills/coversalltm-cocktail.html. Accessed 10 October 2021.
6. RAL Colorchart Web page with Signal Black color reference. https://www.ralcolorchart.com/ral-classic/ral-9004-signal-black. Accessed 10 October 2021.
7. Tate Papers Web Page. https://www.tate.org.uk/research/tate-papers/23/conserving-mark-rothkos-black-on-maroon-1958-the-construction-of-a-representative-sample-and-the-removal-of-graffiti-ink .Accessed 7 August 2022.
8. Hackney S. On Canvas; preserving the structure of paintings. Los Angeles: The Getty Conservation Institute; 2020.
9. Germinario G, van der Werf ID, Sabbatini L. Chemical characterisation of spray paints by a multi-analytical (Py/GC-MS, FTIR, μ-Raman) approach. Microchem J. 2016;124:929–39.
10. Sanmartin P, Cappitelli F, Mitchell R. Current methods of graffiti removal: a review. Constr Build Mater. 2014;71:363–74.
11. Bosi A, et al. Street art graffiti: discovering their composition and alteration by FTIR and micro-Raman spectroscopy. Spectrochim Acta Part A Mol Biomol Spectrosc. 2020;225: 117474.
12. Cortea IM, Ratoiu L, Radvan R. Characterization of spray paints used in street art graffiti by a non-destructive multi-analytical approach. Color Res Appl. 2020;46:183–94.
13. Baglioni M, Poggi G, Benavides YJ, Camacho FM. Nanostructured fluids for the removal of graffiti—a survey on 17 commercial spray-can paints. J Cult Herit. 2018;34:218–26.
14. Pellis G, et al. A multi-analytical approach for precise identification of alkyd spray paints and for a better understanding of their ageing behaviour in Graffiti and urban artworks. J Anal Appl Pyrol. 2022;165: 105576.
15. Mistral Industrial Chemicals web page for Solvent Black 5 dye reference sample. https://mistralni.co.uk/collections/dyes-and-indicators/products/solvent-black-5-nigrosine-spirit. Accessed 10 October 2021.
16. Fast Colours web page for Solvent Black 7. https://www.fastcolours.com/bestoil-black-ob-solvent-black-7-ci-504151-31747-p.asp. Accessed 10 October 2021.
17. Kremer Pigments web page for Solvent Blue 70. https://shop.kremerpigments.com/us/shop/dyes-vegetable-color-paints/94416-solvent-blue-70.html. Accessed 10 October 2021.
18. Tate Conservation Record T01170, unpublished.
19. Dow CHEMCOMP™ Solvent Property Modeling Service description. https://www.dow.com/documents/en-us/compliance/110/110-00656-01-computerized-solvent-modeling.pdf/. Accessed 10 October 2021
20. Hansen CM. The three-dimensional solubility parameter -key to paint component affinities I. -solvents, plasticizers, polymers, and resins. J Paint Technol. 1967;39:104–17.
21. Hansen CM. The Universality of the solubility parameter. Ind Eng Chem Prod Res Dev. 1969;8:2–11.
22. Hansen CM. Hansen solubility parameters: a user's handbook. 2nd ed. Boca Raton: CRC Press; 2007.
23. Hansen Solubility Parameters. https://www.hansen-solubility.com/. Accessed 11 April 2021.
24. Kolorjet Chemical web page. https://www.dyes-pigment.com/solvent-tech1.html. Accessed 10 October 2021.

25. Nakanaishi M, Kawachi N. Ink Composition US4525216 (Patent) 1985.
26. Epsilon Web Page for Solvent Black 7. http://www.epsilonpigments.com/solvent-dyes/nigrosine-black/Solvent-Black-7.html. Accessed 10 October 2021.
27. Epsilon Web Page for Solvent Blue 70. Available from: http://www.epsilonpigments.com/solvent-dyes/metal-complex-solvent-dyes/Solvent-Blue-70.html. Accessed 10 October 2021.
28. Vinothkumar K, Sugumaran T, Venkateshwari S. Electrocoagulation coupled with adsorption for effective removal of eosin yellow and nigrosin dyes in aqueous solution. J Appl Nat Sci. 2019;11:97–106.
29. Phenix A, Wolbers R. Removal of varnish: organic solvents as cleaning agents. In: Stoner JH, Rushfield R, editors. Conservation of Easel Paintings. New York: Routledge; 2012. p. 524–54.
30. Penava DS, Tkalec M. Experimental analysis of the tensile properties of painting canvas. AUTEX Res J. 2015;16:182–95.
31. Schoffstall CW, Fisher RT. Development of the standard numbered cotton duck specification; studies of methods of tests and tolerances. Washington: Department of Commerce; 1924. Technological papers of the U.S. Bureau of Standards volume 18, number 264.
32. Yu C. Natural textile fibres: vegetable fibres. In: Sinclair R, editor. Textiles and fashion: materials, design, and technology. Cambridge: Woodhead Publishing; 2015. p. 29–56.
33. Liang CY, Marchessault RM. Infrared spectra of crystalline polysaccharides. I. Hydrogen bonds in native celluloses. J Polym Sci. 1959;37(132):385–95.
34. Liang CY, Marchessault RM. Infrared spectra of crystalline polysaccharides. IV. The use of inclined incidence in the study of oriented films. J Polym Sci. 1960;43(141):85–100.
35. Gardner KH, Blackwell J. The structure of native cellulose. Biopolymers. 1974;13:1975–2001.
36. Sarko A, Muggli R. Packing analysis of carbohydrates and polysaccharides. III. Valonia cellulose and cellulose II. Macromol. 1974;7(4):486–94.
37. Klemm D, Schmauder HP, Heinze T. Cellulose. In Steinbüchel A, editor. Biopolyme. 2015. https://doi.org/10.1002/3527600035.bpol6010
38. Mantanis GI, Young RA, Rowell RM. Swelling of compressed cellulose fiber webs in organic liquids. Cellulose. 1995;2:1–22.
39. Sczostak A. Cotton linters: an alternative cellulosic raw material. Macromol Symp. 2009;280(1):45–53.
40. Heinze T, El Seoud OA, Koschella A. Principles of cellulose derivatization. In: Heinze T, El Seoud OA, Koschella A, editors. Cellulose Derivatives. Springer: Cham; 2018. p. 259–92.
41. Fan L-T, Ghapuray MM, Lee Y-H. Acid hydrolysis of cellulose. In: Fan L-T, Ghapuray MM, Lee Y-H, editors. Cellulose Hydrolysis. Springer: Berlin; 1987. p. 121–48.

Publisher's Note